A practical guide to estimating magnetization direction from magnetic field data

Foss, C.A.[1]

1. CSIRO Mineral Resources, North Ryde, Australia

ABSTRACT

I advise how to recognize the expression of magnetizations divergent from the local geomagnetic field direction for near-circular magnetic anomalies and how to approximately estimate magnetization direction from those anomalies. I then show with case studies how magnetic field inversion can recover reliable estimates of magnetization direction. I address the major concerns of anomaly separation and source position and shape which set studies of measured magnetic fields apart from the ideal dipole case of Helbig analysis for which there is theoretical proof of process. These case studies illustrate that magnetization direction (a bulk property) can be more reliably estimated from magnetic field data than details such as source shape and depth to top. The main caveat is that a source should be 'compact' which I define as having maximum extent no greater in any direction than twice the closest approach of magnetic field measurement or computation (the case studies presented here show this factor of 2 to be conservative).

INTRODUCTION

The geological interpretation of magnetic field data is the search for distributions of magnetization that are both geologically acceptable and generate fields which successfully match the measured magnetic field. The magnetizations are vector resultants of induced components aligned (in almost all cases) with the local geomagnetic field, and remanent components which generally have an unknown orientation. The ratio of remanent to induced magnetization (the Koenigsberger ratio or 'Q factor') is poorly predictable, and only known from direct measurement. It varies over orders of magnitude between induction-dominated and remanence-dominated magnetizations. A common but unjustified approach in magnetic field interpretation is to ignore the presence of remanent magnetization and search only for models of assumed induced magnetization. This approach is favored in expectation that unknown magnetization direction is a substantial impediment to magnetic field interpretation. In this paper I hope to show that for well-defined anomalies due to compact magnetizations there is no serious difficulty in recovering magnetization direction, and that those magnetization direction estimates are more reliable than many details of the magnetization, such as its shape of distribution or depth to top. A correct estimate of magnetization direction upgrades estimates of all other source parameters (particularly position) and provides valuable information about the age of the geological event which gave rise to that magnetization. A broad review of methods to recover estimates of magnetization is given by Clark (2014).

In one of the early papers on modelling magnetic fields of sources with remanent magnetization, Zietz and Andreasen (1967) noted that at steep geomagnetic inclinations the magnetization direction of sources causing near-circular magnetic anomalies can be broadly estimated from the peak to trough amplitude ratio and azimuth, and Schnetzler and Taylor (1984) investigated extension of this relationship to lower geomagnetic inclinations. In recent years there has been a substantial increase in case studies presenting inversions of magnetic field data that allow a free magnetization direction, but the art of predicting magnetization direction from inspection of magnetic field maps has been largely lost. This restricts interpreters in evaluation of their inversion results. It also adds an unhealthy mystique to magnetic field inversion with free magnetization direction, which is fundamentally little different to inversion of magnetic fields with known (generally assumed) magnetization direction or inversion of gravity fields.

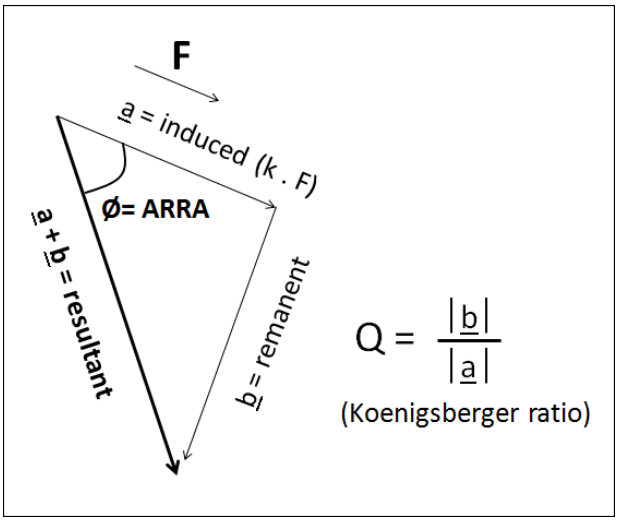

Figure 1 Vector relationships of induced, remanent and resultant magnetizations

Figure 1 illustrates the coplanar relationship between induced, remanent and resultant magnetization. The Koenigsberger ratio is commonly used to quantify the significance of remanent magnetization, but as a scalar it is insufficient to characterize the vector relationship. For instance, without the constraint of measured magnetic susceptibility values, any remanence in or close to the local geomagnetic field direction (such as 'viscous' remanence carried in coarse grained magnetite) cannot be distinguished from induced magnetization (Macnae, 1994). To

more effectively characterize the influence of remanence in magnetic field interpretation I suggest that the Koenigsberger ratio value be supplemented with the apparent resultant rotation angle (ARRA) which measures the departure of the resultant magnetization direction from the local geomagnetic field direction (see Figure 1). Unlike the Koenigsberger ratio, this angle can be estimated directly from magnetic field interpretation.

RECOGNITION OF REMANENCE IN MAGNETIC FIELD IMAGERY

For small departure angles (ARRA < 30°) it may be difficult to visually detect the diagnostic expression of a magnetization direction different to the geomagnetic field, but as the angle increases it becomes more evident that the magnetization is in a different direction to the geomagnetic field. In fields of high geomagnetic inclination changes in declination mostly rotate the dipole axis of the anomaly, and changes in inclination mostly vary the peak to trough amplitude ratio. A simplified diagram of the change of anomaly characteristics with increase of ARRA is shown in figure 2. For ARRA values of 0 to 90° resultant magnetizations are 'normal' and the shape change increases to a maximum, for ARRA values of 90 to 180° resultant magnetizations are 'reverse' and the shape change reduces but with switch of polarity.

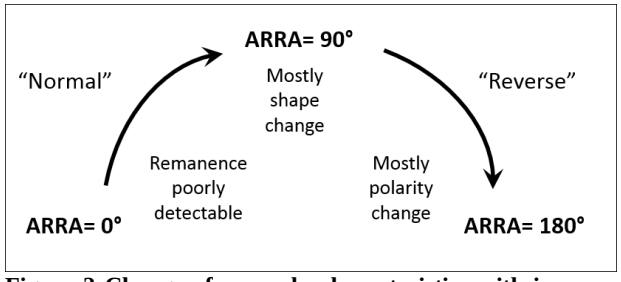

Figure 2 Change of anomaly characteristics with increase of Apparent Resultant Rotation Angle

Figure 3 is a chart of TMI anomalies due to dipoles of different orientation measured in a typical Australian geomagnetic field of inclination -60°. The gaps between examples in the chart are rotations of less than 30°, so it should be possible to find an approximate match to most dipole anomalies. The rows of the chart are constant inclination and mostly show rotation of the dipole axis with declination. The columns of the chart are constant declination (except for the 180° step between rows 3 and 4) and mostly show changes in peak to trough amplitude ratio. For vector component (B_x,B_y, B_z) anomalies this would be a global chart, but TMI anomaly patterns change with geomagnetic inclination because the direction of the TMI vector changes. Figure 4 shows TMI anomalies from the same magnetized dipoles in a steep positive-inclination geomagnetic field (+80°) typical of Canada. The general pattern of variation is similar to that for Australia, but with opposite magnetization polarities. Note that in the steep negative-inclination Australian geomagnetic field the declination of magnetization is approximately in the direction from anomaly trough to peak. For the steep positive-inclination Canadian geomagnetic field the declination of magnetization is in the opposite direction from anomaly peak to trough.

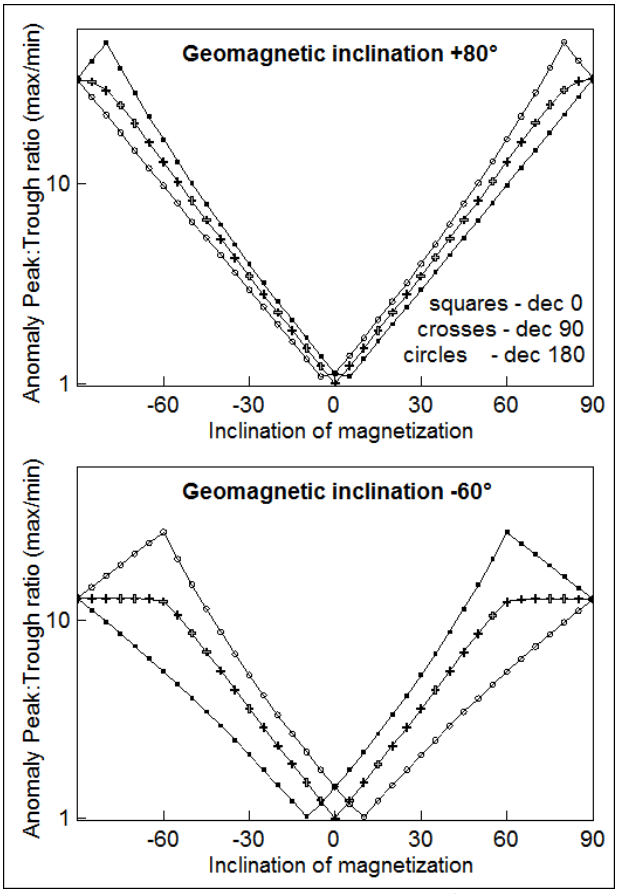

Figure 5 Max:min peak to trough ratios of dipole anomalies in geomagnetic inclinations of (top) -60°, and (bottom) +80°

In steep geomagnetic inclinations magnetizations parallel and anti-parallel to the field have respectively high and low peak to trough ratios, while gentle inclination magnetizations generate anomalies with peak to trough amplitude ratios close to one. This relationship is illustrated in Figure 5, with ratios of less than one inverted. In the +80° inclination field of Canada the inclination of magnetization can be well estimated from the anomaly peak to trough ratio. In the lower -60° inclination field of Australia the relationship is still a reasonable guide to inclination of magnetization, but it is starting to break-down. The vertical component of the field B_z or its vertical gradient B_{zz} provide more robust estimates of magnetization direction (Foss and McKenzie, 2014). Graphical estimates from TMI, B_z or B_{zz} imagery, together with the charts in Figures 3 and 4 summarize the magnetic field expression of magnetization at high southerly and northerly latitudes. Additional charts and alternative relationships for low, mid-southerly and mid-northerly latitude provide a global toolkit for approximate estimation of magnetization direction.

Figures 6A and 6C show induced magnetization dipoles in Australian and Canadian geomagnetic fields respectively, and figures 6B and 6D show the best-fit dipole matches to those anomalies in the alternate geomagnetic field. A typical Australian

induced anomaly (Figure 6A) is strongly positive with a minor negative to the south (towards the pole). A typical Canadian induced anomaly (Figure 6C) is even more strongly positive (because of the higher geomagnetic inclination) with a more subdued negative to the north. To produce a Canadian-like anomaly in an Australia geomagnetic field (Figure 6D) requires an ARRA of 66°, with a southward shift of the source of 9% of its depth. To produce an Australian-like anomaly in a Canadian geomagnetic field (Figure 6B) requires a 63° ARRA with an 11% northward shift. Figures 3 and 4 illustrate that the same magnetizations produce different TMI anomalies in different geomagnetic fields, and Figure 6 illustrates conversely that similar TMI anomalies in different geomagnetic fields are due to differently oriented magnetizations. TMI fields due to induced-only magnetizations also show pronounced differences in anomaly pattern with geomagnetic latitude, with remanent magnetization adding only slightly to this complexity.

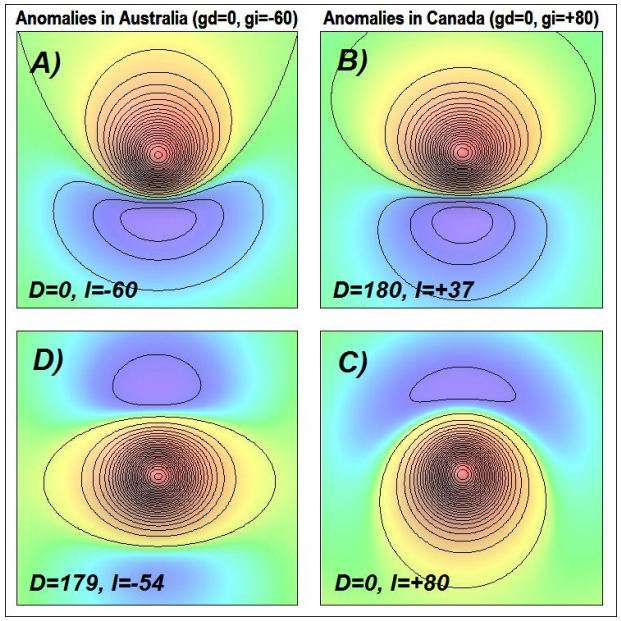

Figure 6 Dipole TMI anomalies: A) induced in a -60° inclination field, C) in a +80° inclination field, B) best-fit to anomaly C) measured in a -60° inclination field, and D) best fit to anomaly A) measured in a +80° inclination field.

Most TMI images used in geological mapping and resource exploration are histogram-equalized and sun-shaded to highlight local variations in the field. These are substantial aids in resolution of geological structure and detail from shallow sources. However, they do not provide the best suited images in which to recognize changes in peak to trough amplitude ratio of anomalies or their dipole alignment. Figure 7 shows anomalies from 4 dipoles of different magnetization direction measured in a magnetic field of -60° inclination. Using the low-shading, contoured image on the left the dipole magnetizations can be roughly estimated from peak to trough relationships described above (or by matching to the anomaly patterns in Figure 3), but the expression of remanent magnetization is much less certain using the conventional strongly shaded image without contours on the right.

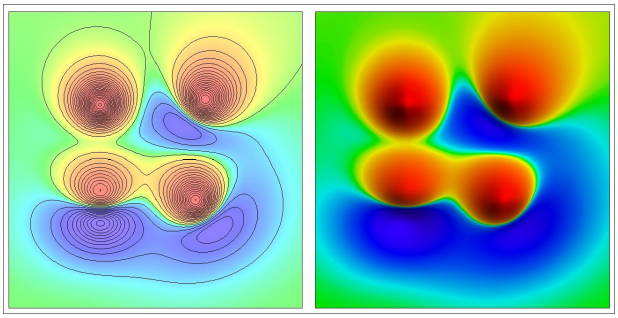

Figure 7 Four TMI dipole anomalies in a -60° inclination field; left with contours, right with sun shading. Magnetizations: NW dipole D=0 I= -90, NE dipole D=045 I= -45, SW dipole D=0 I= -10, SE dipole D=315 I=-45.

REDUCTION TO POLE

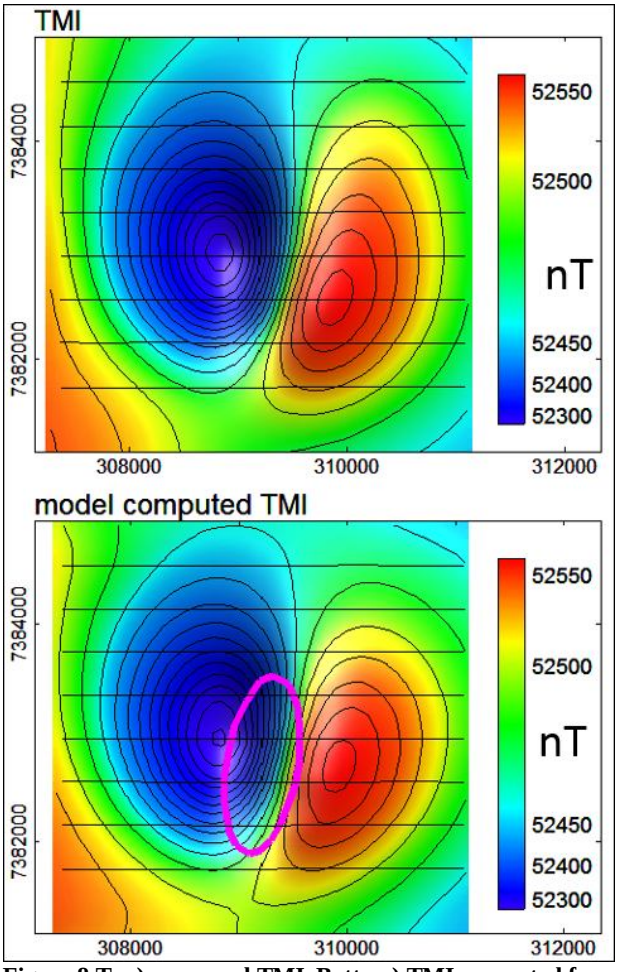

Figure 8 Top) measured TMI, Bottom) TMI computed from an inversion model of the outline shown

Many geologists only use reduced to pole (RTP) imagery. In the steep geomagnetic fields of Canada, and slightly less so in Australia, this is not a major issue because the geomagnetic field is already so steep that the RTP transform produces little change. However, at mid to low geomagnetic inclinations changes on

transformation of the field are substantial (with additional concern of instability of the transform at particularly low inclinations). The intended advantage of RTP is to simplify the shape of anomalies due to non-vertical magnetization measured in a non-vertical field by transform to the field of an identical distribution of vertical magnetization measured in a vertical field. If assumptions are correct, peaks in the field should then lie directly above centers of magnetization. However the conventional RTP transform is invalid if the magnetization direction is not identical to the geomagnetic field direction. This is illustrated in a study of the anomaly imaged in Figures 8 and 9. The top image in Figure 8 shows TMI measured at a geomagnetic inclination of -55°. The azimuth from the anomaly low to peak is 113°, which using the general rules outlined above (and subtracting the geomagnetic declination of +6°) gives a magnetization declination estimate of 107°. The trough to peak ratio of approximately 2 suggests a low to mid positive inclination of about +30°. Using the Figure 3 chart the closest image match to the anomaly is row 2, column 3 with declination 90°, inclination 0°. The bottom image in Figure 8 shows TMI computed from a best-fit inversion model of a steeply plunging elliptic pipe with both spatial parameters and magnetization direction set free in the inversion (I describe through the remainder of the paper how inversions for compact sources are justified). The best-estimated resultant magnetization direction from this inversion is declination 101°, inclination +18°, with an ARRA of 107°. The magnetization direction estimated graphically is less than 15° away from this inversion result, and the estimate made from the chart is only 21° away, illustrating how simple visual checks can provide useful confirmation of inversion results.

Figure 9 shows the standard RTP anomaly (top) and an RTP anomaly using the inversion-estimated magnetization direction (bottom). In this -55° inclination field the standard RTP mostly shifts the anomaly slightly to the south. However, RTP using the inversion-derived magnetization direction substantially changes the anomaly to a near-circular positive-only anomaly as expected for a compact source. Tests for desired RTP output characteristics can be used in magnetization direction searches using trial directions (e.g. Dannemiller and Li, 2006). The peak of the standard RTP is the site of a borehole which does not intersect the magnetization.

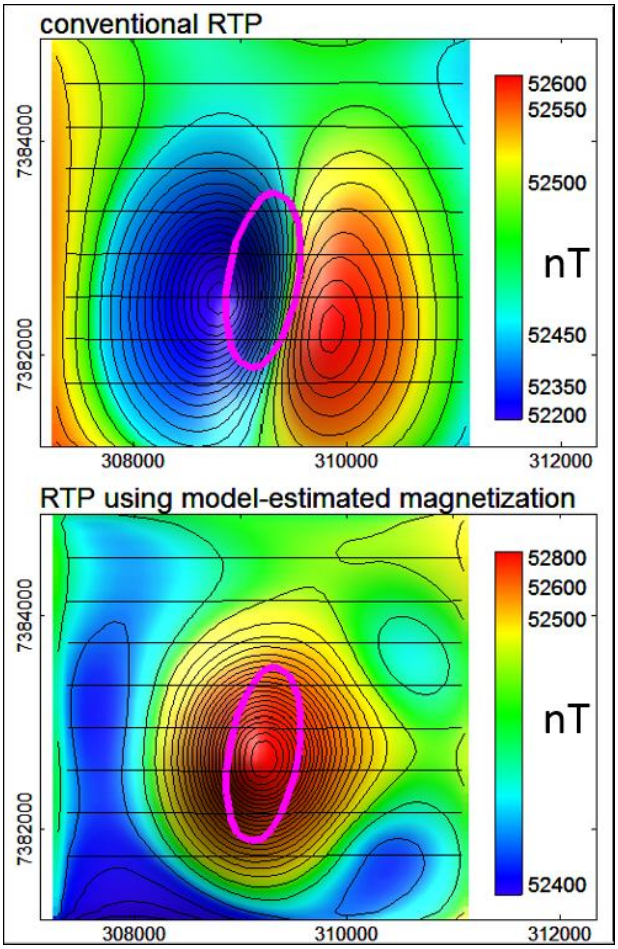

Figure 9 Top) standard RTP, Bottom) RTP using inversion model magnetization direction

The peak of the total gradient anomaly shown in Figure 10 provides a reasonable estimate of the position of the source body because it has only weak sensitivity to magnetization direction (e.g. Roest et al. 1992, Roest and Pilkington 1993, Paine et al 2001, Fullagar and Pears 2015). It appears from Figure 10 that a borehole at the location of the total gradient peak would have an approximately 50% chance of intersecting the body close to its margin. The normalized source strength (Beiki et al. 2012, Clark 2012, Pilkington and Beiki 2013) also shown in Figure 10 has lower sensitivity to magnetization direction than the total gradient. For many anomalies the total gradient and NSS peaks are close to each other, but for this deep body with an ARRA of 107° the NSS peak is significantly closer to the inversion-derived center of magnetization than is the peak in the total gradient.

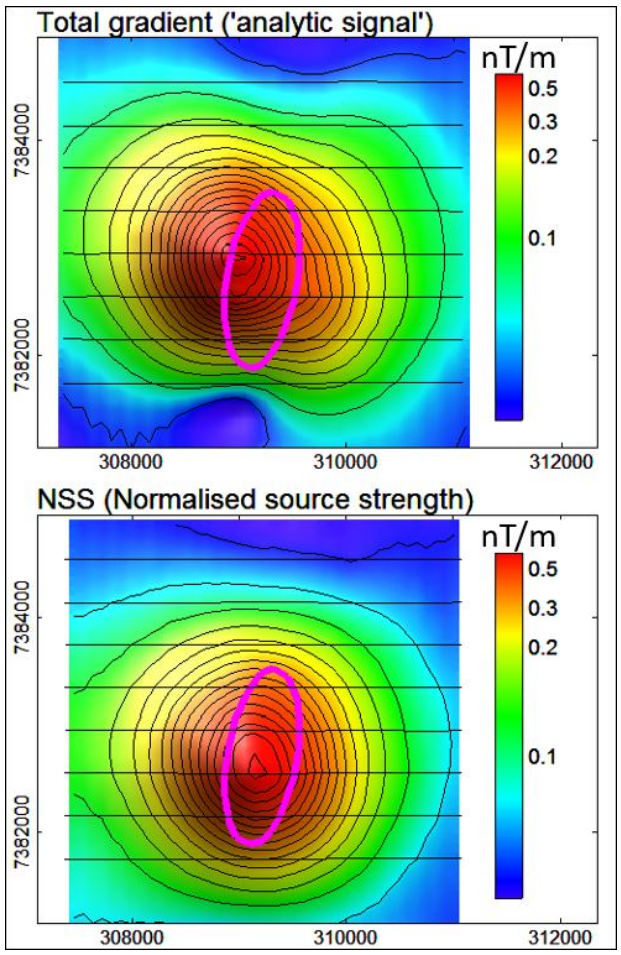

Figure 10: Top) Total gradient, Bottom) NSS. Overlay is best inversion model outline

HELBIG ANALYSIS

The recognition of remanence contributions in magnetic field imagery raises the questions of whether the direction of that magnetization can be recovered, and what can be learnt from it. Also, as noted in the previous study, the process of inverting magnetic field data allowing a free magnetization direction requires validation. The most appropriate reference point from which to address these issues is Helbig analysis which provides an analytic proof of the ability to recover magnetization direction from magnetic field data for the specific case of an isolated field due to a dipole of known location (Helbig 1963). Helbig analysis is illustrated schematically in Figure 11. A TMI anomaly is transformed to component anomalies (Bx, By, Bz). These transforms depend only on the local geomagnetic field direction and are independent of magnetization direction. The moments of those components about the supplied horizontal center of magnetization are derived by numerical integration, and those moments are processed with Helbig's algorithms to determine the amplitude and direction of the magnetic moment. The amplitude term needs correction for the finite integration area (Schmidt and Clark, 1998) but provided the basic assumptions are honored the direction term (which is also the magnetization direction) is stable down to surprisingly small areas of investigation. Several studies have successfully recovered magnetization direction estimates from Helbig analysis of measured magnetic field data (e.g. Schmidt and Clark 1998, Phillips 2005, Foss and McKenzie 2011). Phillips et al. (2007) published an extension to Helbig's analysis which uses the gradient tensor rather than field components. This method is based on approximations but can provide superior results because accumulated errors from the required integrations are more problematic for field components than for their gradients.

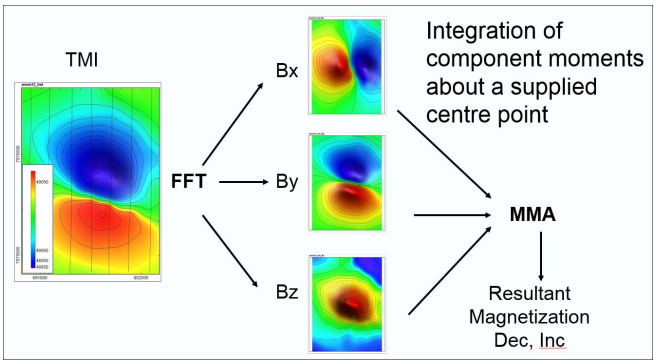

Figure 11 Helbig analysis workflow

Helbig analysis specifically requires an isolated field from a dipole of known horizontal position (a dipole is either a source so small that its shape is inconsequential, or a homogeneous sphere of any size). To extend this analysis to interpretation of measured magnetic fields we have to be confident in the quality of separation of an anomalous (residual) field from the regional field and any overlapping source fields, locate the center of magnetization as well as possible, and be aware of any problems or limitations arising from divergence of the distribution of magnetization from that of an ideal dipole.

MAGNETIC FIELD INVERSION WITH FREE MAGNETIZATION DIRECTION

There is a growing list of case studies showing successful application of various inversion methods allowing a free magnetization direction (e.g. Foss 2006, Lelièvre and Oldenburg 2009, Li et al. 2010, Ellis et al. 2012, MacLeod and Ellis 2013, Pratt et al. 2014). Here I illustrate with case studies how recovery of magnetization directions from magnetic field inversion depends on anomaly separation and source location and shape, and how each of these challenges can be successfully overcome.

Influence of source shape and position

The issue of source shape requires consideration of where the magnetic field is measured or computed. From a sufficient distance any distribution of magnetization can be considered a dipole, with the total magnetization acting as if located at a central point. I use the term 'compact source' to describe a distribution of magnetization which has no extent in any direction greater than twice the closest approach of a magnetic field measurement or computation (this factor of two is conservative - as shown for instance by several of the examples in this paper). For more sophisticated analysis, compaction can be considered independently as horizontal or vertical compaction, using the ratio of maximum horizontal or maximum vertical extent

respectively to minimum separation distance (the anomaly considered in the RTP study above has an extension to proximity ratio of 2.2 and shows very low sensitivity to representation of its shape).

Figure 12 shows a TMI anomaly measured in a survey of the Coompana area of South Australia (Heath et al. 2015, Wise et al. 2016). Also included in the figure are images of TMI forward computed from three inversion models. The anomaly is clearly due to reverse remanent magnetization (Foss et al. 2016), with ARRA for the 3 models between 91° and 93°. The estimated magnetization directions from each inversion are plotted in Figure 13. There is a range of only 3° between directions, with no one direction more than 2° from the mean.

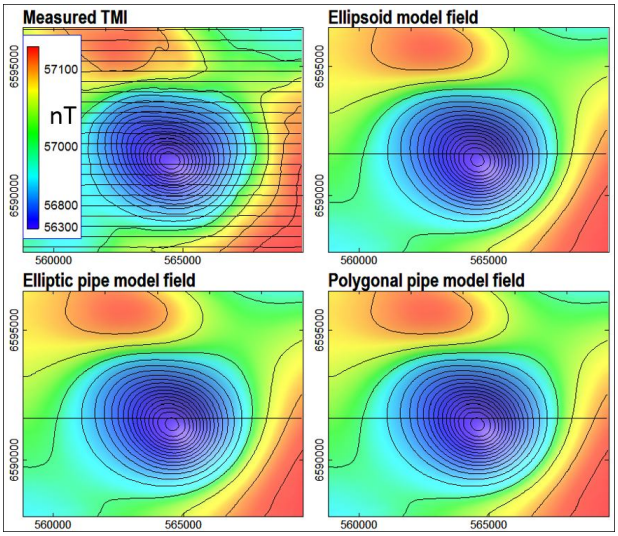

Figure 12 TMI measured (top left) and forward computed from 3 inversion models

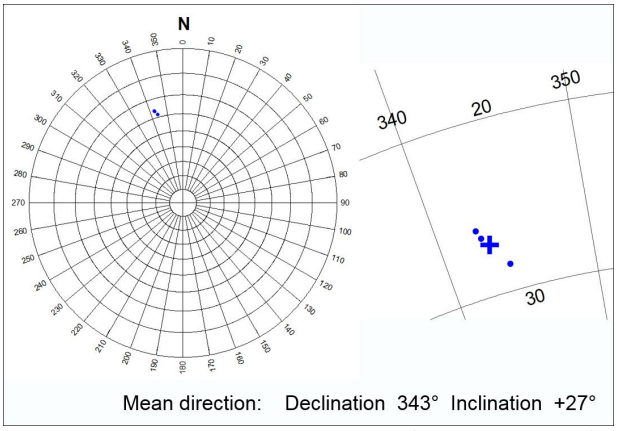

Figure 13 Magnetization directions of the 3 models for Anomaly 266 (cross = mean direction)

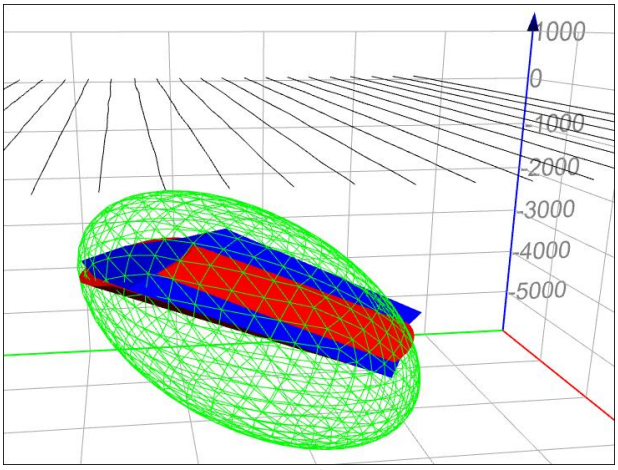

Figure 14 Perspective view of ellipsoid (green), and elliptic (red) and polygonal (blue) pipe models

The inversion models are shown in perspective view in Figure 14. The two horizontal-top pipe bodies of elliptic and polygonal section occupy almost the same space. The ellipsoid model is closely co-centered with those two bodies but has a much larger volume and lower magnetization intensity (giving an almost identical magnetic moment amplitude). The ellipsoid is far from a compact source, with a maximum elongation to proximity ratio of 6.3 (compared to 2.8 and 3.0 for the elliptic and polygonal pipes respectively). However, it is sufficiently close to a sphere to have little sensitivity to volume or magnetization intensity, and can be collapsed to a similar size and magnetization as the pipe bodies with almost no loss in goodness of fit to the data. The most consistent spatial parameters of the bodies are their center coordinates, in particular the horizontal coordinates, showing that the inversions can simultaneously recover estimates of source location as well as magnetization direction. This stability of magnetization direction recovered from the three inversions arises because there is little sensitivity to source shape, and unlike the relationship between volume and magnetization intensity, the pairing between magnetization direction and position is imperfect, allowing the inversion to find consistent values for both individual parameters.

Figure 15 shows sections through the inversion models along the central flight-line. With very small reduction in goodness of fit, depths to the top of all three models can be changed substantially by adjusting volume and magnetization intensity. The two pipe models are considered to provide more appropriate estimates of depth to source because their flat tops are consistent with the geological expectation that they terminate at a sub-horizontal basement surface. However, without that geological guidance there are no grounds to choose between the different models. This example illustrates a general rule that for compact sources there is no fundamental advantage of either parametric or voxel inversion arising from their different treatment of source shape, and that all source shape estimates for compact sources are of low reliability regardless of how simple or complex that shape is.

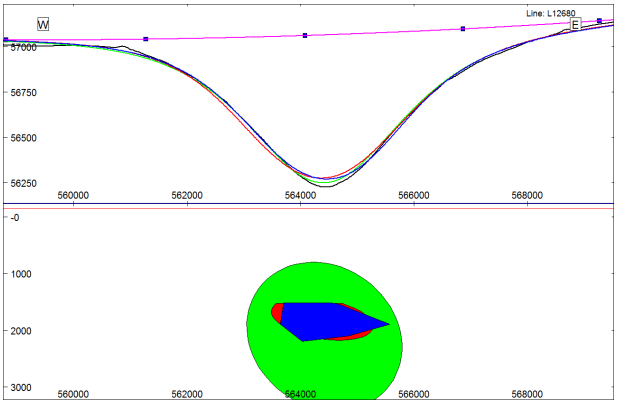

Figure 15 Central flight-line section. Green- ellipsoid, red- elliptic pipe, and blue- polygonal pipe models.

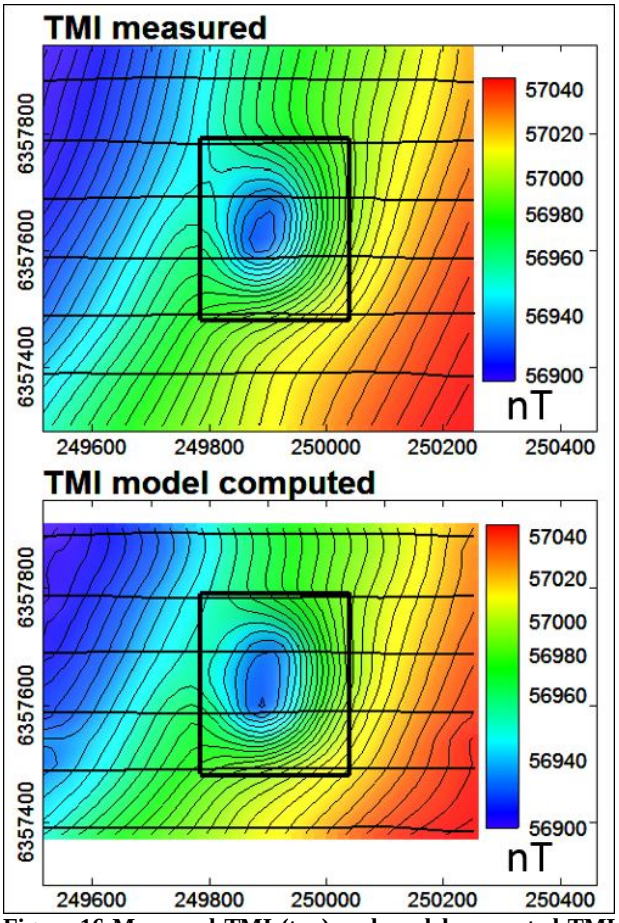

Figure 16 Measured TMI (top) and model computed TMI (bottom) of an anomaly at Rylstone, NSW.

Influence of regional separation

As already explained, anomaly shape described by peak to trough azimuth and peak to trough amplitude ratio is a diagnostic expression of the magnetization direction of a compact source. These two factors are also influenced by gradients in the background regional field, from which the anomaly must be separated (Foss 2006). Any imperfection in the separation threatens the fidelity of magnetization direction estimates subsequently derived from the data. Numerous methods exist to perform regional-residual separations, but there is no dictate that a regional field must have any specific form, and there is no guarantee of a correct separation. Rather, regional-residual separation is essentially an interpretive and non-unique process.

Figure 16 shows measured and model computed fields for a 100 meter line-spaced helming survey over an isolated anomaly in the Rylstone area of New South Wales (geomagnetic inclination -64°). The anomaly is clearly due predominantly to a steep reverse (positive inclination) remanent magnetization and is superimposed on a steep west-to-east regional gradient. Figure 16 shows a section through two separate multi-line inversions, one with an ellipsoid body and the other an elliptic-section pipe. Each inversion produces a close match to the anomaly, and there is a difference in magnetization direction between the two models of less than 3°. The inversion results give an ARRA of 145°. Prior to inversion a regional field was interpreted by selecting samples on each flight-line (as shown in Figure 17) with a smooth low-order polynomial surface best-fitted to those samples. This regional field is subtracted from the measured TMI to give a residual anomaly which is fitted by the inversion. Figure 18 shows the polynomial regional surface and the resulting residual anomaly. The regional separation is well qualified because there is a clear expression of the regional field to all sides of the anomaly. Figure 19 is a clip of both the TMI and residual fields cut to the immediate extent of the anomaly. The TMI image in the clip window still suggests a discrete anomaly due to a compact source superimposed on a positive west-to-east regional gradient, but in this window the two fields overlap completely.

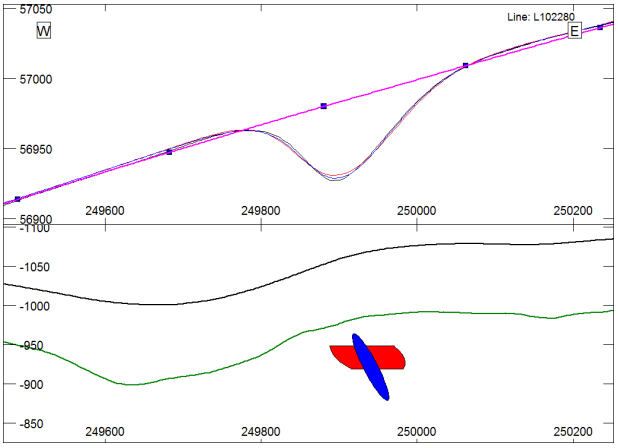

Figure 17 Flight-line section with ellipsoid (blue) and elliptic pipe (red) models, ground (green) and flying height (black). Upper track: measured TMI (black), regional (purple), model computed TMI from the two models (red and blue).

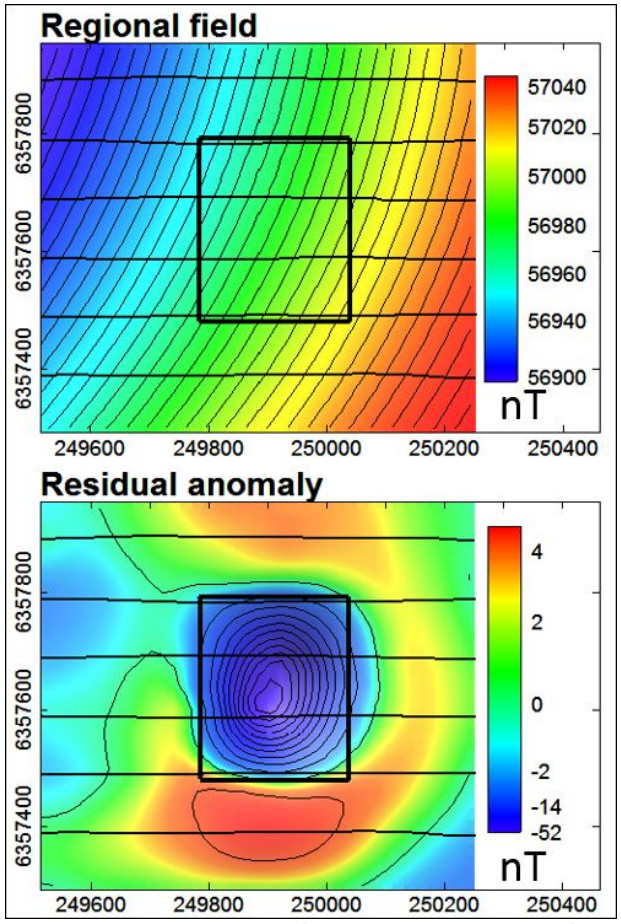

Figure 18 Top) regional field, Bottom) residual from subtraction of regional from measured TMI

Figure 20 shows a section through two models derived from inversion of the residual anomaly within the clip window (the regional fitted to the more extensive data has already been removed). The centers of the bodies are in almost the same location as for the previous inversions. The difference between the two inversion directions is again < 3° and the difference between the mean of these two directions and the mean of the previous inversions is < 7° (see Figure 23). It can be argued that that these inversions of the clipped data are superior, because the more extensive data was used to determine the regional field and then the inversion was focused more tightly on the anomaly, but a more robust estimate of magnetization direction is the mean of all four results. Figure 21 shows a model section derived by inversion of the clipped TMI data allowing only a base-level shift of the regional (included as a parameter in the inversion). This inversion might be attempted if there were no data beyond the clip region from which to detect and estimate the regional gradient. This inversion result is unacceptable because of the very high data misfit, revealing that inversion is able to reject the incorrect premise that the measured field is due only to the field of a discrete source with no regional gradient. The best-fit bodies of the two inversions using only a base-level regional are displaced from the anomaly and elongated in an attempt to simultaneously explain the regional gradient. The mean magnetization of the two models is deflected 66° from the best-estimated direction.

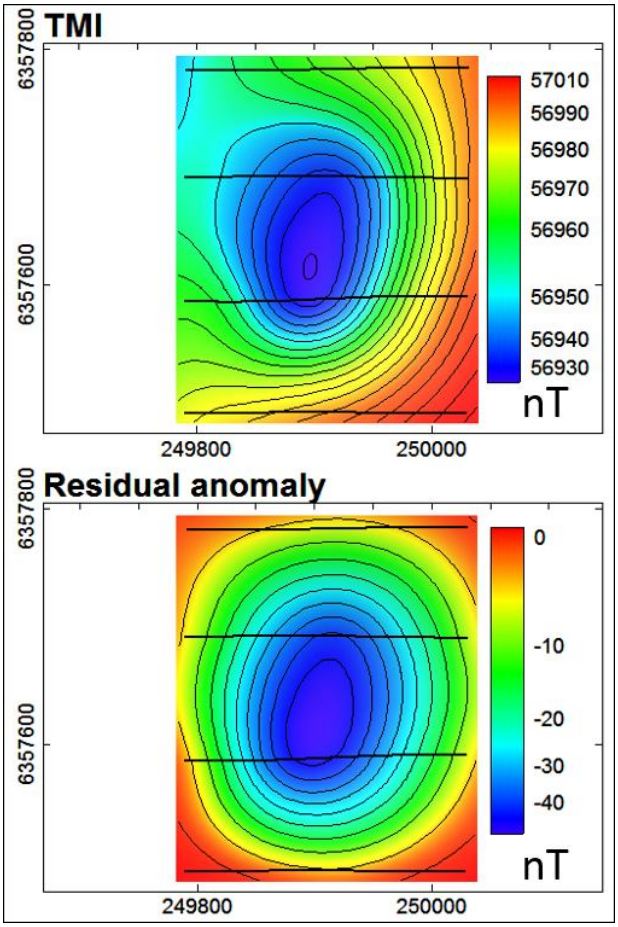

Figure 19 Top) TMI clipped to the anomaly, Bottom) clip of residual anomaly after regional subtraction

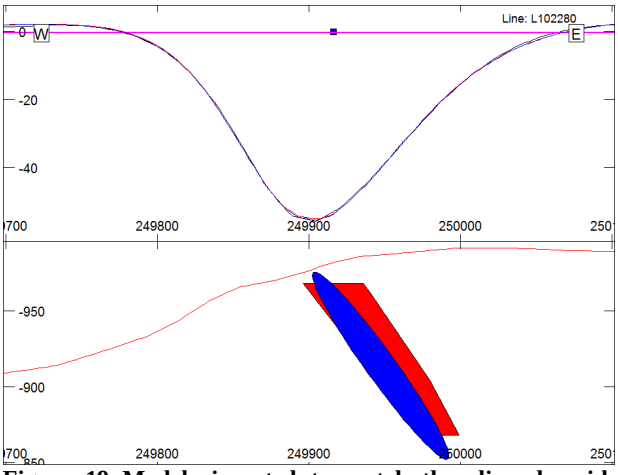

Figure 19 Models inverted to match the clipped residual anomaly with only base-level regional adjustment

Figure 22 shows models derived from inversion of the clipped TMI data in which the inversion was allowed to simultaneously

search for a planar regional gradient and a discrete source. There are reasonable concerns that this process might be computationally unstable, but the tasks of a compact source in explaining the discrete anomaly and a regional in explaining the gradient across the complete window are quite different, and in this case inversions quite successfully resolve both the regional gradient and the source of the residual anomaly. The two inversions with different source geometries again provide consistent results in terms of source location and magnetization direction (with a difference of < 5°). The mean of those magnetization directions is only 10° from the preferred magnetization direction (Figure 23). The goodness of fit of these inversions is high but there is concern about sufficiency of the data as the inversions do not benefit from the more extensive data to define the regional field.

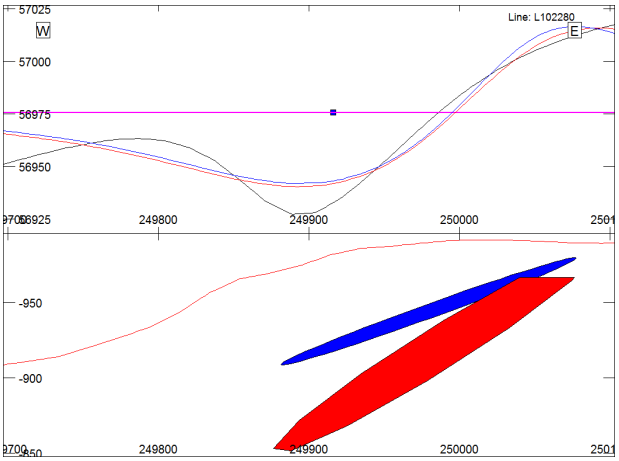

Figure 21 Models inverted to match the clipped TMI with only base-level regional adjustment

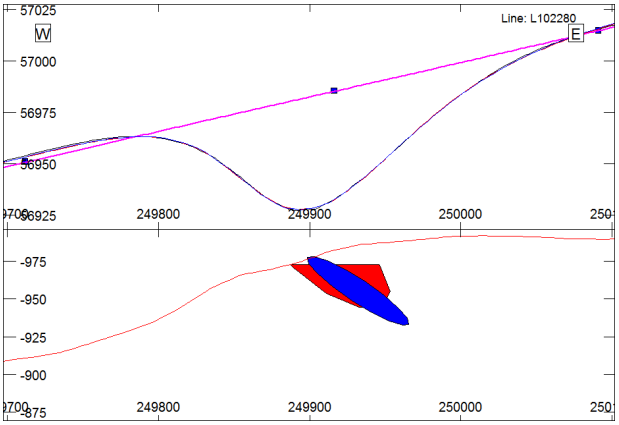

Figure 22 Models inverted to match the clipped TMI with simultaneous planar optimization of the regional

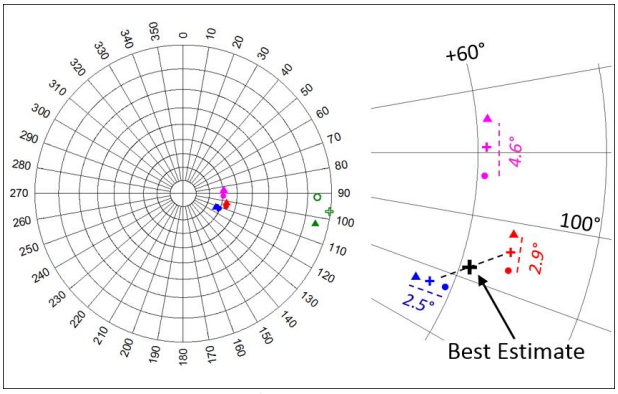

Figure 23 Stereonet of inversion magnetizations: blue - extended TMI, red - clipped residual anomaly, purple - clipped TMI with planar regional, green - clipped TMI with regional level adjustment only (circles - ellipsoids, triangles - elliptic pipes, crosses mean directions)

CONCLUSIONS

I hope I have established in this paper that unknown magnetization direction is not an impediment to magnetic field inversion or interpretation, at least for compact magnetizations which produce anomalies that can be confidently isolated from overlapping and surrounding fields. The recognition in magnetic field images of anomalies likely to be due substantially to remanence is aided by reducing sun-shading and adding a contour overlay. This helps to highlight rotation of the peak to trough alignment of the anomaly and its peak to trough amplitude ratio, both of which are indications of source magnetization direction. Estimates of magnetization direction should always be made from inspection of the magnetic field data prior to running an inversion, so as to have an approximate expectation of the results. Anomaly separation is generally the most critical aspect in determining magnetization direction, and where a regional separation has been performed the regional and residual fields should be imaged to check that there is no unjustified (positive or negative) correlation between them. Estimated distribution of magnetization for compact sources is unreliable but fortunately details of the shape of distribution of a compact magnetization have almost no effect on estimates of its direction. There are trade-offs in inversion between estimated position and magnetization direction so that to obtain a reasonable estimate of either parameter requires a reasonable estimate of both, however this trade-off is imperfect and inversion of well-defined anomalies has the power to individually resolve source position and magnetization direction. A review of the key points in this paper are presented in the summary table below.

ACKNOWLEDGEMENTS

Data for the Coompana anomaly study was provided by the Geological Survey of South Australia from their PACE Frontiers exploration initiative, and I would like to acknowledge my co-workers in that study: Gary Reed, Rian Dutch, Tom Wise and Tim Keeping. The data for the Rylstone study was provided by the Geological Survey of New South Wales. Data for the RTP study was downloaded from the Geoscience Australia GADDS

System. The inversions presented in this paper were performed using ModelVision™ from Tensor Research and the magnetic field map images were generated in Discover PA™ from Pitney Bowes.

REFERENCES

Beiki, M., Clark, D. A., Austin, J. R., and Foss, C. A., 2012, Estimating source location using normalized magnetic source strength calculated from magnetic gradient tensor data: Geophysics, 77, J23–J37. doi:10.1190/ geo2011-0437.1

Clark, D.A., 2012, New methods for interpretation of magnetic vector and gradient tensor data 1: eigenvector analysis and the normalized source strength, *Exploration Geophysics* 43(4) 267-282 http://dx.doi.org/10.1071/EG12020

Clark, D.A., 2014, Methods for determining remanent and total magnetisations of magnetic sources – a review, Exploration Geophysics45, 271-304 http://dx.doi.org/10.1071/EG14013

Dannemiller, N., and Li, Y., 2006, A new method for determination of magnetization direction: Geophysics, 71, L69–L73. doi:10.1190/1.235 6116

Ellis, R. G., de Wet, B., and Macleod, I. N., 2012. Inversion of magnetic data for remanent and induced sources: 22nd ASEG Conference and Exhibition, Extended Abstracts, 1–4.

Foss, C.A., 2006, Evaluation of strategies to manage remanent magnetization effects in magnetic field inversion: 76th Annual International Meeting, SEG, Expanded Abstracts, 938–942.

Foss, C.A., and B. McKenzie, 2011, Inversion of anomalies due to remanent magnetisation: An example from the Black Hill Norite of South Australia: Australian Journal of Earth Sciences, 58, 391–405, doi: 10.1080/08120099.2011.581310.

Foss, C.A., and B. McKenzie, 2014, Bz and Bzz peak to trough ratios and azimuths as a rapid means to map magnetization directions – a method based on pioneering studies by Zietz and Andreasen (abstract): GSA Annual Meeting, paper 15-10. 2014. https://gsa.confex.com/gsa/2014AM/finalprogram/abstract_247836.htm

Foss,C.A., Reed, G., Keeping, T., Wise, T.W., and Dutch, R.A., 2016a, Looking into a 'blue hole' – resolving magnetization and structure from the complex negative Coompana anomaly, South Australia, ASEG Extended Abstracts, 1-8.

Fullagar, P. K., and G. A. Pears, 2015, Remanent magnetisation inversion: 24th ASEG International Geophysical Conference, ASEG, Extended Abstracts.

Heath, P., Reed, G., and Katona, L., 2015, 2015 Coompana airborne survey, MESA Journal, 79(4), 18-21.

Helbig, K., 1963, Some integrals of magnetic anomalies and their relation to the parameters of the disturbing body: Zeitschrift für Geophysik, 29, 83–96.

Lelièvre, P. G., and D. W. Oldenburg, 2009, A 3D total magnetization inversion applicable when significant, complicated remanence is present: Geophysics, 74, no. 3, L21–L30, doi: 10.1190/1.3103249.

Li, Y., Shearer, S., Haney, M., and Dannemiller, N., 2010, Comprehensive approaches to the inversion of magnetic data affected by remanent magnetization: Geophysics, 75, L1–L11. doi:10.1190/1.3294766

MacLeod, I. N., and Ellis, R. G., 2013, Magnetic vector inversion – a simple approach to the challenge of varying direction of rock magnetization: A Forum on the Application of Remanent Magnetisation and Self Demagnetisation Estimation to Mineral Exploration: 23rd ASEG Conference and Exhibition, Melbourne.

Macnae, J., 1994, Viscous magnetization: misleading Koeningsberger's Q: SEG Technical Program Expanded Abstracts, 456–458.

Paine, J., M. Haederle, and M. Flis, 2001, Using transformed TMI data to invert for remanently magnetised bodies: Exploration Geophysics, 32, 238–242, doi: 10.1071/EG01238.

Phillips, J., 2005, Can we estimate total magnetization directions from aeromagnetic data using Helbig's formulas: Earth Planets Space, 57, 681–689, doi: 10.1186/BF03351848.

Phillips, J.D., Nabigian, M.N., Smith, D.V., and Li, Y., 2007, Estimating locations and total magnetization vectors of compact magnetic sources from scalar, vector, or tensor magnetic measurements through combined Helbig and Euler analysis, SEG Technical Program extended abstracts, 26, 770-774, doi.org/10.1190/1.2792526

Pilkington, M., and M. Beiki, 2013, Mitigating remanent magnetization effects in magnetic data using the normalized source strength: Geophysics, 78, no. 3, J25–J32, doi: 10.1190/geo2012-0225.1.

Pratt, D. A., McKenzie, K. B., and White, A. S., 2014, Remote remanence determination (RRE), Exploration Geophysics, 45, 314-323.

Roest, W., and M. Pilkington, 1993, Identifying remanent magnetization effects in magnetic data: Geophysics, 58, 653–659, doi: 10.1190/1.1443449.

Roest, W. R., J. Verhoef, and M. Pilkington, 1992, Magnetic interpretation using the 3-D analytic signal: Geophysics, 57, 116–125, doi: 10.1190/1.1443174.

Schmidt, P.W., and Clark, D. A., 1998, The calculation of magnetic components and moments from TMI: a case study from the Tuckers igneous complex, Queensland: Exploration Geophysics, 29, 609–614. doi:10.1071/EG998609

Schnetzler, C.C. and P.T. Taylor, 1984, Evaluation of an observational method for estimation of remanent magnetization, Geophysics, 49, 282-290, doi: 10.1190/1.1441660

Wise, T.W., Pawley, M.J., and Dutch, R.A., 2016, Preliminary interpretations from the 2015 Coompana aeromagnetic survey, MESA Journal 79(4), 22-30.

Zietz, I., and Andreasen, G.E., 1967, Remanent magnetization and aeromagnetic interpretation: in Mining Geophysics, 2, SEG, Tulsa, 569-590.

1	The external magnetic field of a body is a function of its resultant (remanent plus induced) magnetization.
2	Koenigsberger ratio values calculated from rock magnetic measurements suggest that remanent magnetization contribute substantially to most measured magnetic field variations.
3	Many, and possibly most measured magnetic anomalies are due to magnetizations with some departure from the local geomagnetic field direction.
4	For magnetic field studies of magnetization, the Koenigsberger ratio should be supplemented with a measure of the angular rotation of magnetization away from the local geomagnetic field, here termed the apparent resultant rotation angle (ARRA).
5	Helbig's 1963 proof that the direction of a dipole magnetization can be recovered from magnetic field analysis is the fundamental basis for investigation of the magnetization direction of any compact source.
6	Extension of Helbig's proof to studies of geological magnetizations requires reliable isolation of an anomaly from overlapping fields, accurate determination of the center of magnetization, and appropriate correction for any influence of shape and plunge.
7	At steep geomagnetic inclinations the peak to trough azimuth and amplitude ratio indicate magnetization direction. These characteristics are more clearly expressed in magnetic field images with subdued sun-shading and contour overlays.
8	Vertical component (Bz) images provide more reliable indication of magnetization direction than TMI images, particularly in moderate to low geomagnetic inclination fields.
9	The standard RTP is invalid for magnetizations not in the geomagnetic field direction, but the transform can be adjusted to accept other magnetization directions.
10	The total gradient transform has low sensitivity to magnetization direction, and the Normalized Source Strength (NSS) has even less.
11	The exact distribution of a compact magnetization has little effect on estimation of its magnetization direction.
12	Because shape detail is relatively unimportant, parametric and voxel inversions of identical anomaly separations should provide essentially identical resultant magnetization direction estimates.
13	Position and estimated magnetization direction of a compact source are closely linked. In inversion, an error in one causes an error in the other, but for well-defined anomalies both position and magnetization direction can both be resolved.
14	Anomaly (regional-residual) separation is commonly the most critical aspect in determining magnetization direction.
15	Where inversion has itself been used to perform an anomaly separation it is important to review images of the regional and residual fields to ensure that the separation is acceptable.
16	Estimation of magnetization direction is relatively robust because it is a bulk characteristic rather than a detail (such as depth to top, or shape), and also because it does not have a particularly close pairing with any other parameter or parameter set (as for instance do intensity of magnetization and volume, which are so closely paired that there is generally little sensitivity to either value, only to their product).

Table 1 Summary of key points presented in this paper

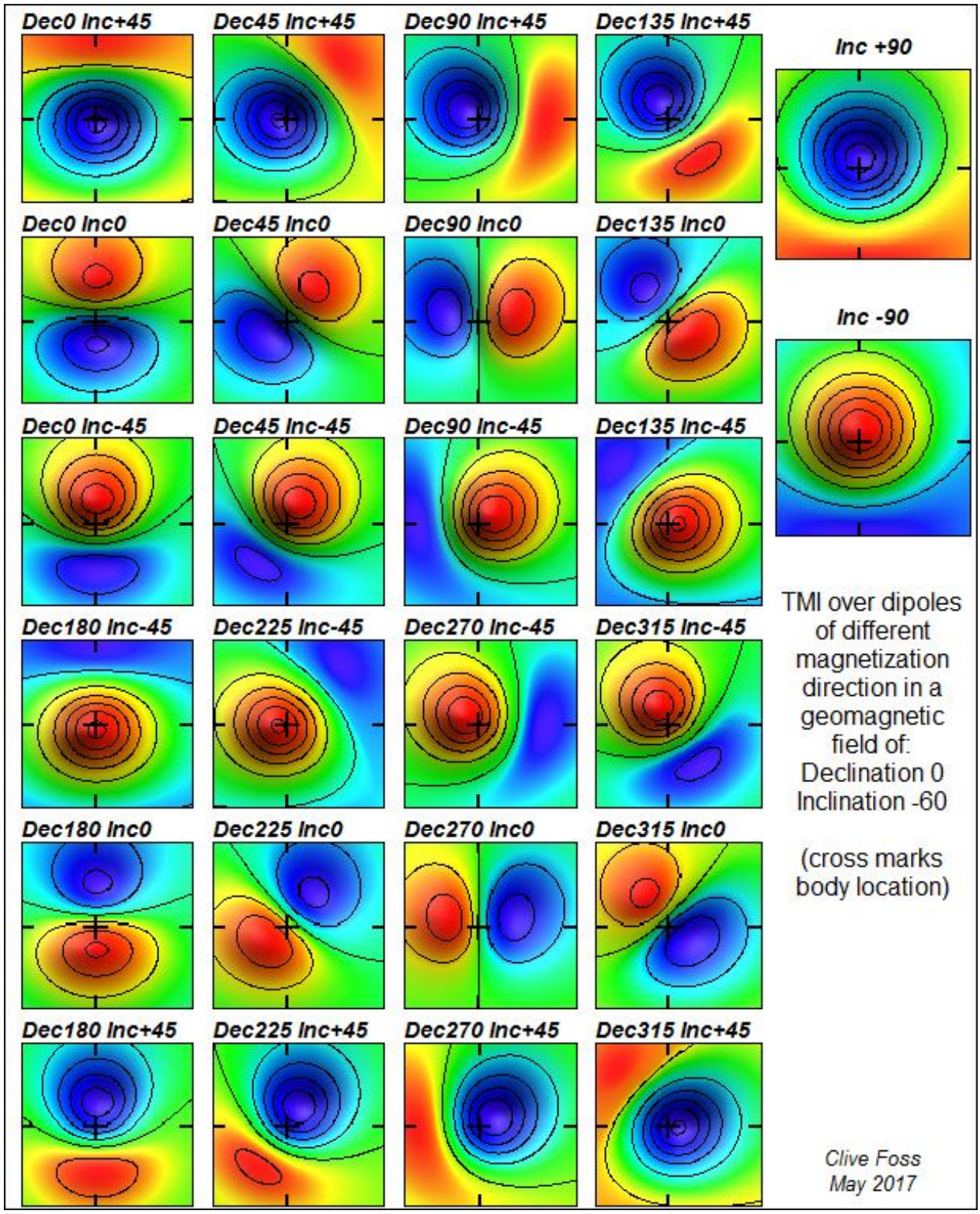

Figure 3 TMI anomalies due to dipoles of specified magnetization in a geomagnetic field of inclination -60°

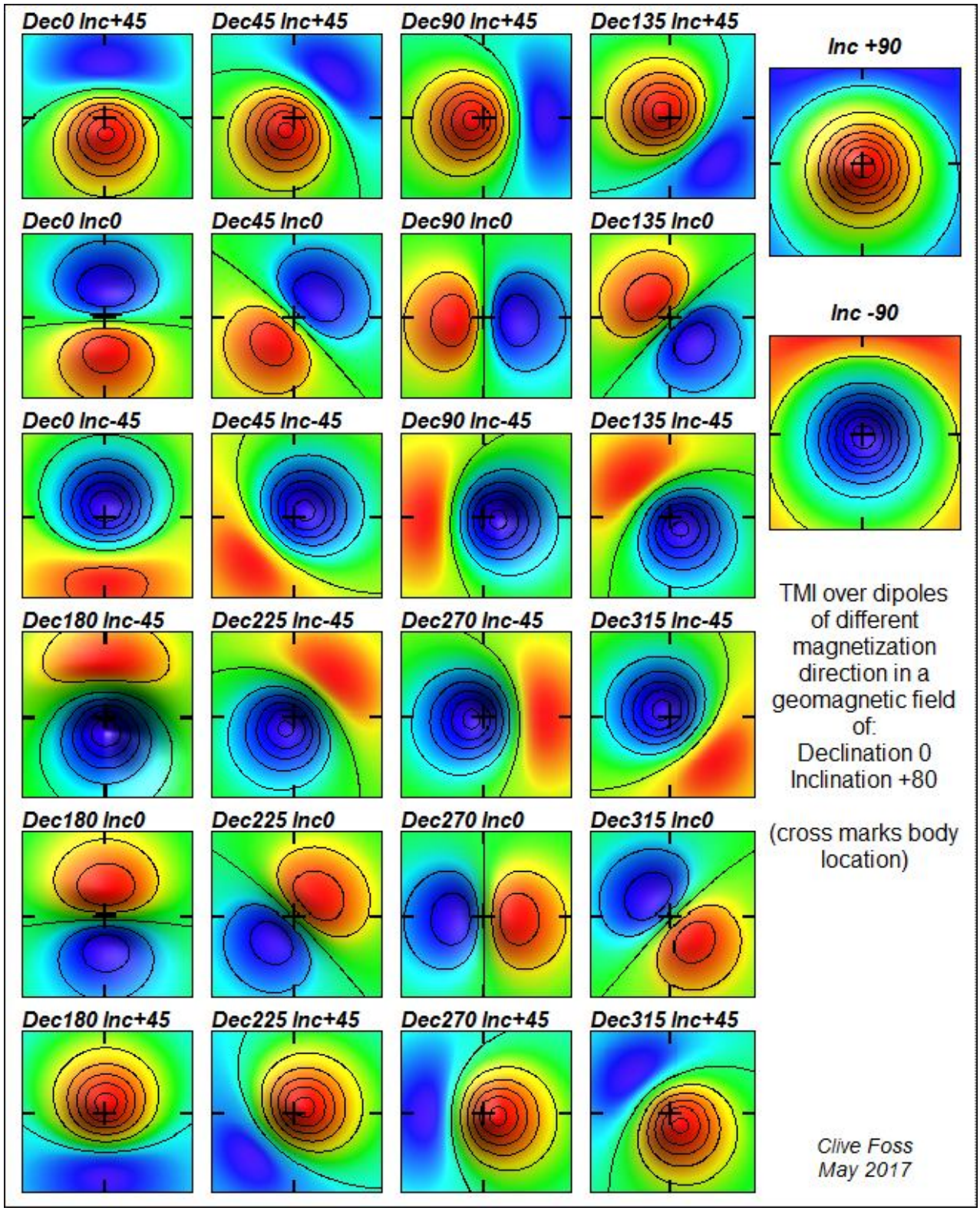

Figure 4 TMI anomalies due to dipoles of specified magnetization in a geomagnetic field of inclination +80°